

More Emission Cones: Multi-frequency Simulation of the Pulse Profiles of PSR J0437–4715

Guo-Jun Qiao ^{*}, Xu-Dong Wang, Hong-Guang Wang and Ren-Xin Xu

Department of Astronomy and CAS-PKU Joint Beijing Astrophysics Center, Peking University, Beijing 100871

Received 2002 February 9; accepted 2002 April 20

Abstract Pulsar radio emission beams have been studied observationally for a long time, and the suggestion is that they consist of the so-called core and conal components. To reproduce these components is a challenge for any emission model, and that the pulse profile of pulsars changes with frequency presents even a greater challenge. Assuming a local surface magnetic structure (to produce the core or central beam) and a global dipole magnetic field (to produce the conal beams), Gil & Krawczyk (1997) applied curvature radiation to the pulse profile simulation of PSR J0437–4715 (hereafter the GK model). Here we present an alternative multi-frequency simulation of the same profiles within the framework of the Inverse Compton Scattering (ICS) model. It is obtained from our simulation (1) that besides the core, the inner cone and the outer cone, there is an outer-outer cone; (2) that the emission components of the core and cones evolve strongly with frequency. Some important differences between the ICS model and the GK model are discussed, which need to be tested by further observations.

Key words: pulsar: general — radiation mechanisms: ICS — pulsar: individual (PSR J0437–4715)

1 INTRODUCTION

The shape of the mean pulse profile of pulsars is usually extremely stable, which provides much information of the underlying emission mechanism. Rankin (1983, 1990, 1993) proposed that the emission beam is composed of two distinct types of emission components, known as core and (one or two) conal components. She pointed out that the two components have different properties. Lyne & Manchester (1988) while confirming the different properties, argued that there is only one (rather than two) conal component, and that two distinct emission mechanisms are not necessary. This debate has lasted for many years. Some other authors suggested that pulsar beams may consist of up to three or even four nested cones (e.g. Mitra & Deshpande

^{*} E-mail: gjn@pku.edu.cn

1999; Gil & Sendyk 2000; Gangadhara & Gupta 2001). They argued that the structure of pulsar beams is conal but not patchy (Gil & Krawczyk 1996). Han & Manchester (2001) considered that observations support the patchy beam model, in which the mean beam shape represents the properties of the emission mechanism and the observed pulse components result from emission sources distributed randomly across the beam. No firm conclusion on this issue has been reached so far. It is possible that the real pulsar emission beam is the convolution of a “patchy” source function and a “window” function (Manchester 1995). The “windows” may be composed of a central core component plus one or more nested “conal” components, and sparking takes place in each “window” and shows up as “patchy” sources in the observations (Qiao et al. 2001).

The inner vacuum gap model (Ruderman & Sutherland 1975, hereafter RS75), has come closest to enable a comparison between observations and theories. Unfortunately it can only produce the hollow emission beam. To create core and conal emission beams, Gil et al. (2000) proposed a modified non-stationary inner vacuum polar gap model. The key feature of this model is the assumption that at, or near the magnetic polar cap center there exists a local sunspot-like magnetic field structure, which causes sparking and results in the core component. From the center to the edge of the gap there are two to three circular rings and sparking takes place there. The central spark is fixed, while the other sparks perform a slow drift $\mathbf{E} \times \mathbf{B}$ around it. Qiao and co-workers (e.g. Qiao 1992; Qiao & Lin 1998, hereafter Paper I; Xu et al. 2000, hereafter Paper III; Qiao et al. 2001, hereafter Paper II) used the Inverse Compton Scattering (ICS) model to reproduce the various emission beams; in this model the inner gap sparks and an associated low frequency wave are needed.

Besides reproducing core and conal emission beams, a greater challenge to the many current emission models is how to reproduce the pulse profiles, especially their variation with frequency. It is clear that the evolution of the pulse profile with frequency provides valuable information on the emission beams, and in turn puts further constraints on the current theoretical models. Sieber (1997) considered the geometry of the hollow-cone model, and assumed a central core to reproduce the pulse profile changes with frequency only in geometrical terms. Paper I presents a model to reproduce the core and conal emission beams. A set of systematic simulations for the evolutionary behavior of the pulse profiles of many normal pulsars are presented in Paper II within the framework of the ICS model, in which the variations of the core, inner cone and outer cone components with frequency are studied. Can we produce an additional outer cone component and infer its frequency dependence in the model?

PSR J0437–4715 presents a real challenge for the current models of pulsar emission not only for its strong evolutionary behavior with frequency, but also because it shows seven components at some frequencies in its mean profiles. In this paper, within the framework of the ICS model, the pulse profiles of this pulsar at four radio frequencies are simulated. We give a basic picture of the ICS model in Section 2. The simulations are presented in Section 3. Our discussion and conclusions are given in Section 4.

2 THE INVERSE COMPTON SCATTERING (ICS) MODEL

2.1 The Basic Physical Picture

The basic picture of the ICS model is as follows (Qiao 1992, Paper I): a low frequency wave ($\nu_0 \sim 10^5 \text{ s}^{-1}$) is assumed to be excited near the pulsar polar cap region by the periodic breakdown of the inner gap (Ruderman & Sutherland 1975), and is assumed to propagate

outwards in the open field line area up to some limited heights. These low energy photons are inverse Compton scattered by the secondary particles produced in pair cascades (with Lorentz factor $\gamma \sim 10^2 - 10^4$), and the up-scattered radio photons just provide the observed radio emission from the pulsar. Recent detailed polar cap “mapping” by Deshpande & Rankin (1999) indicates that periodic storms induced by gap breakdown are indeed happening at least in some pulsars, which provides a solid observational foundation for the ICS model.

2.2 Basic Formulae for the Emission Beams

For most pulsars, $B \ll B_q = 4.414 \times 10^{13}$ Gauss at points near or far from the surface of the neutron star. The Lorentz factors satisfy $\gamma = 1/\sqrt{1-\beta^2} \gg 1$, $\beta = v/c \sim 1$. The outgoing photons are produced by inverse Compton scattering between the low frequency photons and the outgoing high energetic particles. The frequency of the scattered photon reads (Qiao 1992; Paper I),

$$\nu \simeq 2\gamma^2\nu_0(1 - \beta \cos \theta_i), \quad (1)$$

where θ_i is the incoming angle between the direction of particle motion and the incoming photons, ν_0 is the frequency of the low frequency wave produced in the inner gap sparking. For a dipole magnetic field line, we have

$$r = R_e \sin^2 \theta, \quad (2)$$

where, r is the distance of the scattering point from the center of the neutron star, $R_e = \lambda R_c$, λ is a constant for a given dipole magnetic field line, $\lambda \geq 1$, $\lambda = 1$ corresponding to the last open field line. $R_c = Pc/2\pi$ is the radius of the light cylinder, P the period of the pulsar, c the light speed, θ the polar angle of the scattering point with respect to the magnetic axis. The angle θ_i can be expressed as (Paper I):

$$\cos \theta_i = \frac{2 \cos \theta + (R/r)(1 - 3 \cos^2 \theta)}{\sqrt{(1 + 3 \cos^2 \theta)[1 - 2(R/r) \cos \theta + (R/r)^2]}}, \quad (3)$$

where R is the radius of the pulsar. The angle between the radiating direction (along the magnetic field) and the magnetic axis, θ_μ , has a simple relation with θ (Paper I):

$$\cot \theta_\mu = \frac{2 \cot^2 \theta - 1}{3 \cot \theta}. \quad (4)$$

The Lorentz factor of the particles will change with distance. It is assumed that γ has the following relation with r (this will be discussed in the point 4 of Section 4):

$$\gamma = \begin{cases} \gamma_0 [1 - \xi(r - R)/R_e], & (R < r < R + R_e/\xi), \\ \eta [(r - (R + R_e/\xi))/R], & (R + R_e/\xi < r < R_e), \end{cases} \quad (5)$$

where both ξ and η are constants and we will point out later that they may indicate the energy “decrease” and “increase” processes of particles, γ_0 is the initial Lorentz factor of the high energy particles.

The relation between the longitudinal semi-width $\Delta\phi$ of the beam and its angular radius θ_μ is given by (e.g. Gil et al. 1984):

$$\sin^2(\theta_\mu/2) = \sin^2(\Delta\phi/2) \sin \alpha \sin(\alpha + \beta) + \sin^2(\beta/2), \quad (6)$$

where α is the inclination angle, β is the impact angle, $2\Delta\phi$ is the pulse width in longitude. Equations (1)–(6) are the basic formulae for emission beams of a pulsar, on which our simulation is based.

3 A MULTI-FREQUENCY SIMULATION OF PSR J0437–4715

PSR J0437–4715 is a close and bright millisecond pulsar, with a period of 5.75 ms. In our simulation, we adopt Gil’s inclination angle $\alpha = 20^\circ$ and impact angle $\beta = -4^\circ$ (Gil et al. 1997). Other parameters used in the simulation are: $\nu_0 \sim 0.1$ MHz, $\gamma_0 = 7800$, $\lambda = 6$ (corresponding to the polar angle of sparks $\theta = 0.41\theta_p$), $R = 10$ km, $\xi = 15$, $\eta = 100$. $R + R_e/\xi \simeq 200$ km. The beam radius θ_μ at a given frequency is calculated by Eqs. from (1) to (6), giving the locations of the emission components. Then we make Gaussian fits to the observational data, taking the height and the width of the Gaussian function as inputs.

Figure 1 is a sketch of the beam-frequency relation for PSR J0437–4715. The mean pulse profiles of PSR J0437–4715 at four frequencies are displayed in Fig. 2. The left column shows the observational results. The following features can be seen: its mean pulse profiles evolve strongly with frequency; seven emission components appear at 1.52 GHz; the width of the pulse profile expands as the frequency increases. At some frequencies, it even occupies over 280° of longitude. The right column shows the simulation results. From Fig. 2 one may see that our simulation can reproduce the observed complex behavior of this pulsar. Figure 3 gives a more detailed comparison between the observation and the simulation.

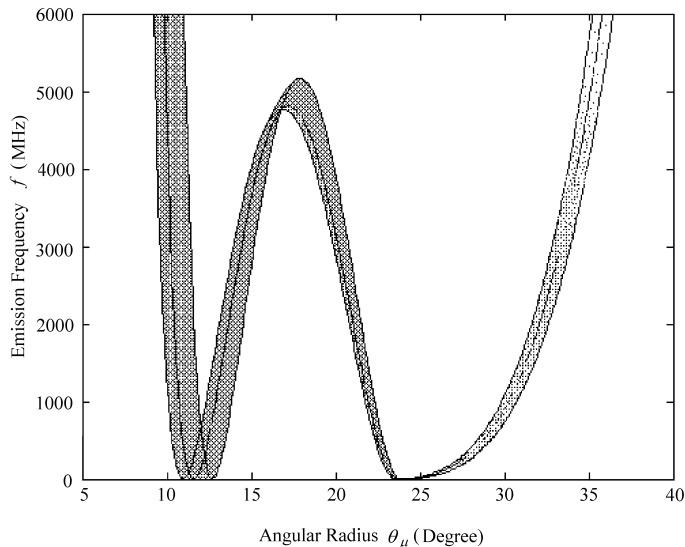


Fig. 1 Beam-frequency figure of PSR J0437–4715. Different color deepness stands for different intensity in this figure.

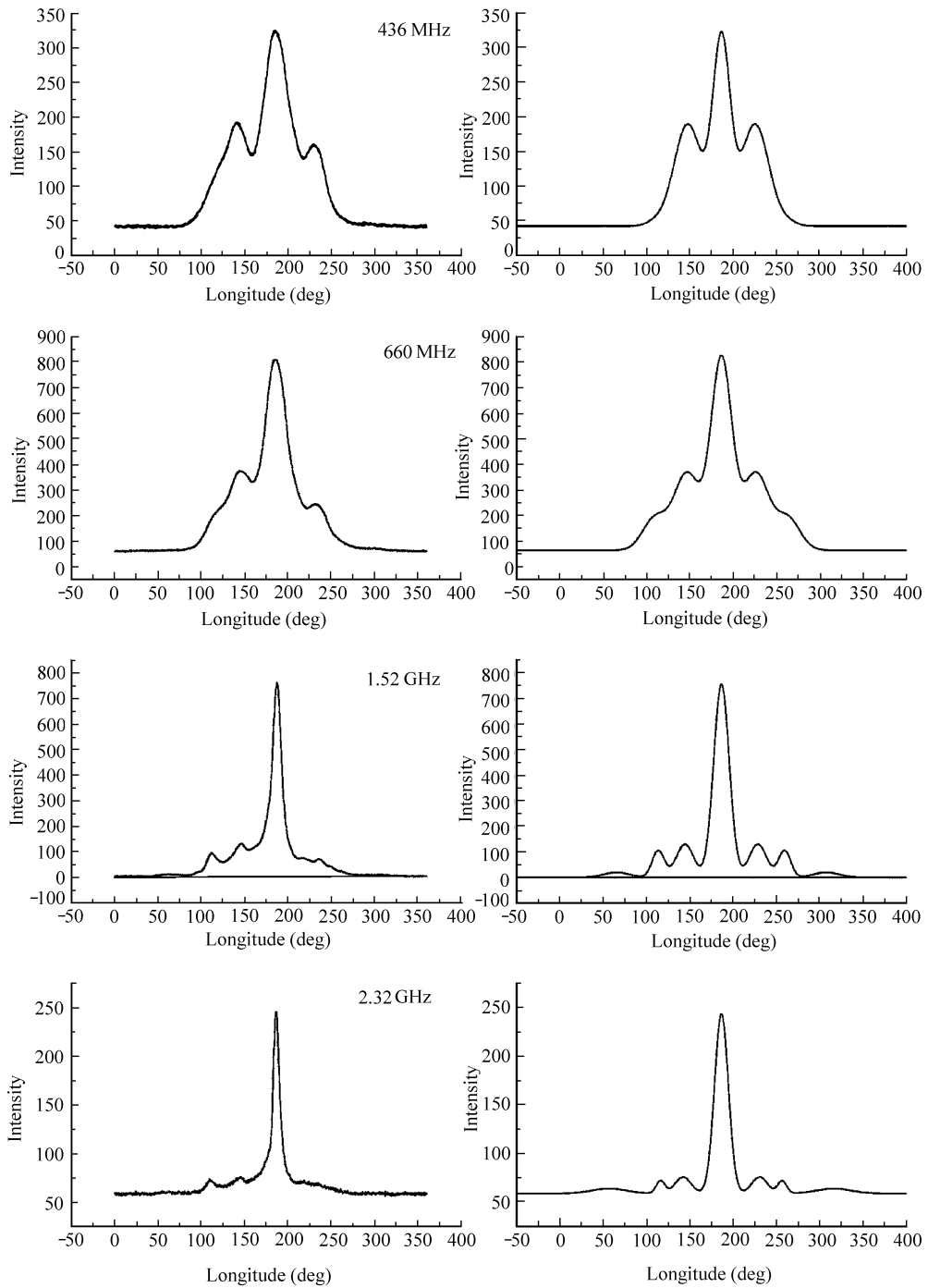


Fig. 2 Multi-frequency simulation of PSR J0437–4715 at 436, 660, 1520, 2320 MHz; the evolutionary behavior of this pulsar with frequency is clearly displayed. The left column corresponds to the observational results, the right column to the simulation.

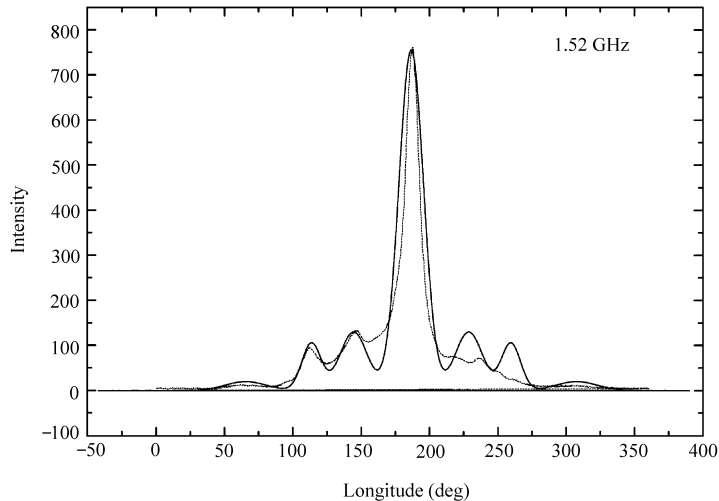


Fig. 3 A more detailed comparison between the observational data at 1.52 GHz (dashed lines) and the simulation (solid lines).

4 DISCUSSION AND CONCLUSIONS

(1) To reproduce the special structure of the mean pulse profile of PSR J0437–4715 and its evolutionary behavior with frequency is a real challenge for current radiation models. In this paper, within the framework of the ICS model, we reproduce the core-cone beam structure of PSR J0437–4715, with an additional outer-outer cone component. A multi-frequency simulation of the pulse profiles of the pulsar is also made, and the result can be compared with the observations.

(2) The basic formula Eq. (1) used in our simulation is derived from mono-energetic distribution of particles. In more realistic cases, particles should have a certain energy distribution (e.g., power law), and the locations of sparks in the polar cap are also distributed in some way (e.g. Gaussian). To compare with the observed integrated pulse profiles, the Gaussian curve is adopted for the various emission components, which can reflect all the effects above (Paper II; Wu et al. 1998).

(3) The shape of the pulse profile of PSR J0437–4715 varies dramatically with the observing frequency. The core and conal components can be fitted with our simulations on the whole, but the asymmetry of some of the observed profiles cannot be well fitted. This observational feature needs a separate study that includes relative longitudinal phase shift (see Xu et al. 2001a).

(4) In our simulations, the form of Eq. (5) is adopted, in which the value of the Lorentz factor decreases at first and then increases. Why does the Lorentz factor behave like this? In fact, when the particles move along field lines, their energy will be lost owing to scattering with the thermal photons (Xia et al. 1985; Sturmer 1995; Zhang et al. 1997) and the low frequency wave (Paper I), but the area in which this energy loss occurs is very limited (see Zhang et al.

1997). For most areas the energy loss is negligible. It therefore seems that the change of γ in Eq. (5) is actually an observational effect, which can be seen from Eq. (1) as follows. The shape of the “beam-frequency figure” is just the result of the competition between two factors, the angular factor $(1 - \beta \cos \theta_i)$ and the energy factor γ^2 (see Fig. 1). In our simulations a homogeneous Lorentz factor is used. In fact, out of the inner gap the particles should have an energy distribution, such as $N(\gamma) = N_0 \gamma^{-g_0}$, which leads to different values of γ playing the dominant role in different places. We can see from Eq. (1) that, for a given observing frequency ν , the value of γ must be smaller at the outer than the inner cone. This is because the value of $(1 - \beta \cos \theta_i)$ at the outer cone is larger than at the inner cone (it reaches the smallest value between the core and the inner cone). Since the number density of particles is greater for small than for large γ , this, together with the coherent effect¹ means that the particles with lower values of γ should play the dominant role in higher locations. This is what we use in our simulations: $\gamma = \gamma_0 [1 - \xi(r - R)/R_e]$, for $R < r < R + R_e/\xi$. However, in higher places such as $(R + R_e/\xi) < r < R_e$, some acceleration processes will play important roles.

The theory of particle acceleration has been investigated for many years. There are two kinds of accelerators: the polar cap and the outer gap accelerators. For the polar cap accelerator, if the ion binding energy of the neutron star crust is large enough, a vacuum inner gap accelerator will work; otherwise, the space-charge limited flow accelerator will work. Instead of neutron stars, if pulsars are bare strange stars, the vacuum gap accelerator will work (Xu & Qiao 1998; Xu et al. 1999, 2001b). In this paper we concentrate on the vacuum gap accelerator. For this kind of accelerator, the acceleration by $\mathbf{E} \cdot \mathbf{B}$ (the electric field is parallel to the magnetic field) in the inner gap is considered only, but out of the gap there are still some acceleration processes because the space-charge limited flow acceleration process also takes place outside the inner gap. This is because, although close to the inner gap, the charge density of the out-flowing particles, ρ , and the charge density in the static magnetosphere of the neutron star, ρ_{gj} , are equal, in higher places $(\rho - \rho_{gj}) \neq 0$, and the “second acceleration” process will take place (see Arons & Scharlemenn 1979; Harding & Muslimov 1998; Goldreich & Julian 1969). A detailed analysis will be given separately. In the present work, the parameter η measures this effect and its value is determined by the observations. When the particles pass through these zones, they will be accelerated. This acceleration is responsible for the additional emission branch (the right most branch of the ‘W’), in Fig. 1, corresponding to an outer-outer cone component, as compared with the “normal” “beam-frequency figure” in Papers I and II. For this branch, as the frequency gets higher, the emission place gets higher, and the emission intensity gets weaker due to the decreasing number densities of both high energetic particles and photons. The outer-outer cone component will not be observable up to a certain distance (corresponding to some higher frequency).

(5) The pulse profiles of PSR J0437–4715 are simulated by both the GK model and the ICS model. The differences between these two models are as follows:

a) According to the ICS model (fig. 5 of paper I) and the data analysis (Rankin 1993), the different emission beams are emitted from different heights; according to the GK model, different emission beams originate from different “hot-spots” in the polar cap, and the different emission beams (core, inner cone, outer cone and so on) are emitted continuously from any distance in principle, whether they are strong or weak. These two scenarios lead to different predictions: in the GK model, every emission component, including the outer-outer cone component, should

¹ The particles in a coherent volume are the product of the coherent volume ($\propto \nu^{-3}$). See Mitra & Deshpande 1999 and references therein.

be stronger at a higher than at a lower frequency; whereas in the ICS model the outer-outer cone component is emitted from the highest position of emission zones: it should be weaker than the other components at any given frequency, and more so at higher frequencies, as is observed to be the case.

b) Besides the pulse profiles of PSR J0437–4715, many other kinds of pulse profiles of pulsars can be reproduced within the framework of the ICS model (Paper II). As pointed out by GK, the emission mechanism of millisecond pulsars is the same as that of typical pulsars. If this is the case, then other types of frequency behavior, observed in other pulsars than PSR J0437–4715, could also be produced by the GK model. We are looking forward to seeing such fittings.

Acknowledgements We are grateful to Dr. Han J. L., Mr. Xue Y. Q. for many helpful discussions with them. This work is partly supported by NSF of China, and the Research Fund for the Doctoral Program Higher Education.

References

- Arons J., Scharlemann E. T., 1979, *ApJ*, 231, 854
 Deshpande A. A., Rankin J. M., 1999, *ApJ*, 524, 1008
 Gangadhara R. T., Gupta Y., 2001, *ApJ*, 555, 31
 Gil J., Gronkowski P., Rudnicki W., 1984, *A&A*, 132, 312
 Gil J., Krawczyk A., 1996, *MNRAS*, 280, 143
 Gil J., Krawczyk A., 1997, *MNRAS*, 285, 561
 Gil J., Sendyk M., 2000, *ApJ*, 541, 351
 Goldreich P., Julian W. H., 1969, *ApJ*, 157, 869
 Han J. L., Manchester R. N., 2001, *MNRAS*, 320, L35
 Harding A. K., Muslimov A. G., 1998, *ApJ*, 508, 328
 Lyne A. G., Manchester R. N., 1988, *MNRAS*, 234, 477
 Manchester R. N., 1995, *J. Astrophys. Astr.* 16, 107
 Mitra D., Deshpande A. A., 1999, *A&A*, 346, 906
 Qiao G. J., 1992, In: T. H. Hankins, J. M. Rankin, J. A. Gil, eds., *IAU Colloq. 128, The Magnetospheric Structure and Emission Mechanisms of Radio Pulsars*, Zielona Gora, Poland: Pedagogical Univ. Press, p.195
 Qiao G. J., Lin W. P., 1998, *A&A*, 333, 172 (Paper I)
 Qiao G. J., Liu J. F., Zhang B., Han J. L., 2001, *A&A*, 377, 964 (Paper II)
 Rankin J. M., 1983, *ApJ*, 274, 333
 Rankin 1990, *ApJ*, 352, 247
 Rankin 1993, *ApJ*, 405, 285
 Ruderman M. A., Sutherland P. G., 1975, *ApJ*, 196, 51
 Sieber W., 1997, *A&A*, 321, 519
 Sturmer S. J., 1995, *ApJ*, 446, 292
 Wu X. J., Gao X. Y., Rankin J. M., Xu W., Malofeev V. M., 1998, *AJ*, 116, 1984
 Xia X. Y., Qiao G. J., Wu X. J., Hou Y. Q., 1985, *A&A*, 152, 93
 Xu R. X., Liu J. F., Han J. L., Qiao G. J., 2000, *ApJ*, 535, 354 (paper III)
 Xu R. X., Qiao G. J., 1998, *Chin. Phys. Lett.*, 15, 934
 Xu R. X., Qiao G. J., Zhang B., 1999, *ApJ*, 522, L108
 Xu R. X., Xu J. W., Qiao G. J., 2001a, *Chin. J. Astron. Astrophys.*, 1, 152
 Xu R. X., Zhang B., Qiao G. J., 2001b, *Astropart. Phys.*, 15, 101
 Zhang B., Qiao G. J., Han J. L., 1997, *ApJ*, 491, 891